Chemical Proteomics Hot Paper

International Edition: DOI: 10.1002/anie.201903472
German Edition: DOI: 10.1002/ange.201903472

The Natural Product Elegaphenone Potentiates Antibiotic Effects against *Pseudomonas aeruginosa*

*Weining Zhao, Ashley R. Cross, Caillan Crowe-McAuliffe, Angela Weigert-Munoz, Erika E. Csatary, Amy E. Solinski, Joanna Krysiak, Joanna B. Goldberg, Daniel N. Wilson, Eva Medina, William M. Wuest, and Stephan A. Sieber**

Abstract: *Natural products represent a rich source of antibiotics that address versatile cellular targets. The deconvolution of their targets via chemical proteomics is often challenged by the introduction of large photocrosslinkers. Here we applied elegaphenone, a largely uncharacterized natural product antibiotic bearing a native benzophenone core scaffold, for affinity-based protein profiling (AfBPP) in Gram-positive and Gram-negative bacteria. This study utilizes the alkynylated natural product scaffold as a probe to uncover intriguing biological interactions with the transcriptional regulator AlgP. Furthermore, proteome profiling of a Pseudomonas aeruginosa AlgP transposon mutant provided unique insights into the mode of action. Elegaphenone enhanced the elimination of intracellular P. aeruginosa in macrophages exposed to sub-inhibitory concentrations of the fluoroquinolone antibiotic norfloxacin.*

Innovative antibacterial drugs are urgently needed to address the current antibiotic crisis. Natural products have been a reliable source and the majority of marketed drugs are based on this class.[1] Looking at current modes of action, a limited number of hot spot targets such as cell wall, nucleotide, and protein biosynthesis have been evolutionarily selected. Furthermore, the constant use of antibiotics has resulted in multiple-resistance mechanisms, calling for novel drugs that address unprecedented and resistance-free pathways.[2] An intriguing new perspective for developing next-generation antibiotics is based on attenuating the production of toxins, which would decrease the severity of infections and minimize the development of resistance.[3] In order to rapidly identify such innovative modes of action, several strategies for target deconvolution are applied. A common method is to select for resistant strains and corresponding sequencing to reveal mutations in the target gene.[4] However, this classical method falls short when it comes to indirect resistance mechanisms (e.g. drug efflux). Moreover, molecules that reduce virulence but do not kill bacteria are difficult to address via this method. Thus, chemical proteomics, such as activity-based protein profiling (ABPP), have been applied.[5] While some antibiotics, including β-lactams, covalently modify their target, a large number of natural products bind reversibly.[6] For the latter class, functionalization with a photocrosslinker is required in order to withstand the conditions of mass spectrometry (MS)-based proteomics, which is referred to as affinity-based protein profiling (AfBPP).[7] A major drawback of the corresponding photoprobes is often a drop in biological activity when these modifications are introduced to the parent scaffold. Inspired by a phenotypic screen of synthetic compounds deliberately utilizing the benzophenone photocrosslinker as an active moiety, we searched for antibacterial natural products bearing this core motif.[8] A large fraction of natural antibacterials exhibit phenolic structures including the benzophenone-motif-containing elegaphenone (**EL**), a minimally characterized antibiotic produced by the plant St. John's Wort, used for diverse medical applications (Figure 1 A).[9] Here we show

[*] W. Zhao, A. Weigert-Munoz, J. Krysiak, Prof. Dr. S. A. Sieber
Department of Chemistry
Center for Integrated Protein Science Munich (CIPSM)
Technische Universität München
Lichtenbergstraße 4, 85747 Garching (Germany)
E-mail: stephan.sieber@tum.de

A. R. Cross, J. B. Goldberg
Division of Pulmonary, Allergy & Immunology, Cystic Fibrosis and Sleep, Department of Pediatrics
Emory University School of Medicine
Atlanta, GA (USA)

A. R. Cross
Microbiology and Molecular Genetics Program
Graduate Division of Biological and Biomedical Sciences
Emory University
Atlanta, GA (USA)

A. R. Cross, J. B. Goldberg, W. M. Wuest
Emory + Children's Center for Cystic Fibrosis and Airway Disease Research, Emory University School of Medicine
Atlanta, GA (USA)

C. Crowe-McAuliffe, D. N. Wilson
Institute for Biochemistry and Molecular Biology
University of Hamburg
20146 Hamburg (Germany)

E. E. Csatary, A. E. Solinski, W. M. Wuest
Department of Chemistry, Emory University
Atlanta GA (USA)

J. B. Goldberg, W. M. Wuest
Emory Antibiotic Resistance Center, Emory University
Atlanta, GA (USA)

E. Medina
Helmholtz Center for Infection Research
Inhoffenstraße 7, 38124, Braunschweig (Germany)

Supporting information and the ORCID identification number(s) for the author(s) of this article can be found under: https://doi.org/10.1002/anie.201903472.

The mass spectrometry proteomics data have been deposited with the ProteomeXchange Consortium via the PRIDE partner repository with the dataset identifier PXD010476.

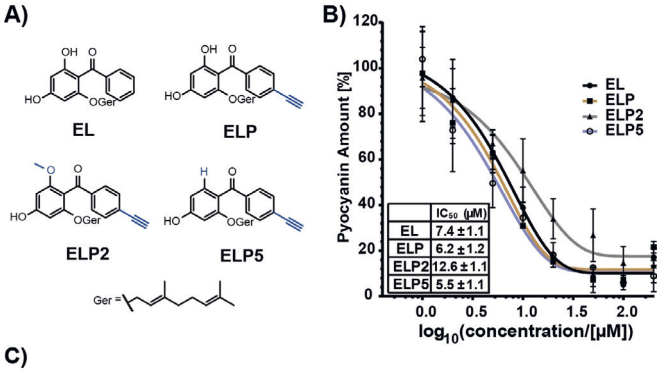

C)

Strain \ MIC (μM)	EL	ELP	ELP2	ELP5
S. aureus NCTC 8325	5	5	>100	37
S. aureus USA300	5	7.5	>100	9
S. aureus Newman	5	5	>100	2.6
S. aureus Mu50	12.5	12.5	>100	>100
S. aureus VA409044	12.5	6.25	>100	12.5
S. aureus BK097296	12.5	12.5	>100	6.25
E. faecalis V583	7.5	7.5	>100	4
E. rivorum S299	12.5	12.5	>100	12.5
L. Monocytogenes EGD-e	5	3.8	>100	4
E. coli BW25113 *ΔbamBΔtolC*	75-150	>300	>300	>300
P. aeruginosa PAO1	>200	>200	>200	>200

Figure 1. A) Structures of elegaphenone (**EL**) and derivatives. B) The amount of extracellular pyocyanin in *P. aeruginosa* PAO1 upon treatment with elegaphenone and derivatives in a dose-dependent manner. The data is based on two biological experiments with technical triplicates. C) MIC values of elegaphenone derivatives in different pathogenic bacterial strains. Lack of growth inhibition is highlighted in gray. *E. coli* BW25113 *ΔbamBΔtolC* is a hyperpermeable *E. coli* strain.[13]

that **EL** not only kills *Enterococcus faecalis*, but also attenuates virulence of *Pseudomonas aeruginosa.* AfBPP utilizing the photoreactive core scaffold paired with whole proteome studies provide unique insights into the mode of action. Additionally, the combination of **EL** with subinhibitory concentrations of norfloxacin enhanced the elimination of intracellular *P. aeruginosa* by macrophages.

EL was prepared following a route inspired by the synthesis of olympicin A (Scheme S1).[10] For the corresponding probes the alkyne tag was directly appended to the monosubstituted benzene ring in the *para* position. For this we devised a synthesis of derivatives that bear an alkyne tag (**ELP**), exhibit a methylated hydroxyl group (**ELP2**), or lack a hydroxyl group (**ELP5**) on the adjacent benzene ring (Figure 1 A). **ELP** was synthesized by Friedel–Crafts acylation of *p*-bromobenzoic acid chloride with trimethoxybenzene followed by Sonogashira coupling with ethynyltrimethylsilane. Demethylation and subsequent bisprotection of two hydroxyl groups allowed the selective incorporation of a geranyl group in the *ortho* position. Global deprotection under acidic conditions provided **ELP** in 42% yield (Scheme 1). Probes **ELP2** and **ELP5** were obtained via a similar strategy with slight modifications (Schemes S2 and S3).

With the natural product and three probes in hand, we first evaluated the biological activity against representative Gram-positive and Gram-negative reference strains, that is, *E. faecalis* and *P. aeruginosa*, respectively. In line with previous reports, **EL** exhibited antibiotic activity against *E. faecalis* as well as other Gram-positive strains, including *Staphylococcus aureus* and *Listeria monocytogenes* with MIC values ranging from 5–12.5 μM (Figure 1 C).[9]

ELP and **ELP5** showed comparable potency while **ELP2** was completely inactive. None of the compounds inhibited *P. aeruginosa* growth and even growth of a hyperpermeable strain of *Escherichia coli* could only be affected by **EL** at high concentrations. However, given the structural similarity of **EL** to natural phenolic inhibitors of *P. aeruginosa* quorum sensing, we tested the compounds against *P. aeruginosa* toxin production.[11] We decided to monitor the levels of pyocyanin, a toxin important during lung infection in cystic fibrosis (CF) patients.[12] Satisfyingly, **EL** and its corresponding probes revealed strong inhibition of pyocyanin production, with IC_{50} values ranging between 5.5 ± 1.1 and 12.6 ± 1.1 μM (Figure 1 B). In addition, **EL** and **ELP5** also reduced the level of pyoverdine, another *P. aeruginosa* toxin, albeit at much higher concentrations (Figure S1 A). Interestingly, the benzophenone core scaffold by itself neither inhibited *E. faecalis* growth, nor reduced *P. aeruginosa* pyocyanin production, emphasizing the importance of the substitution pattern of the natural product for activity (Figure S1 B).

In order to elucidate the corresponding cellular pathways addressed by **EL** and analogues, we performed AfBPP utilizing the alkynylated **EL** photoprobes. *E. faecalis* bacterial cells were incubated with its closest derivative **ELP**, irradiated, lysed, and clicked to biotin azide (Figure 2 A). The probe-labeled proteome was enriched on avidin beads and peptides were released for LC-MS/MS analysis via tryptic digestion. MS analysis was performed via isotopic dimethyl

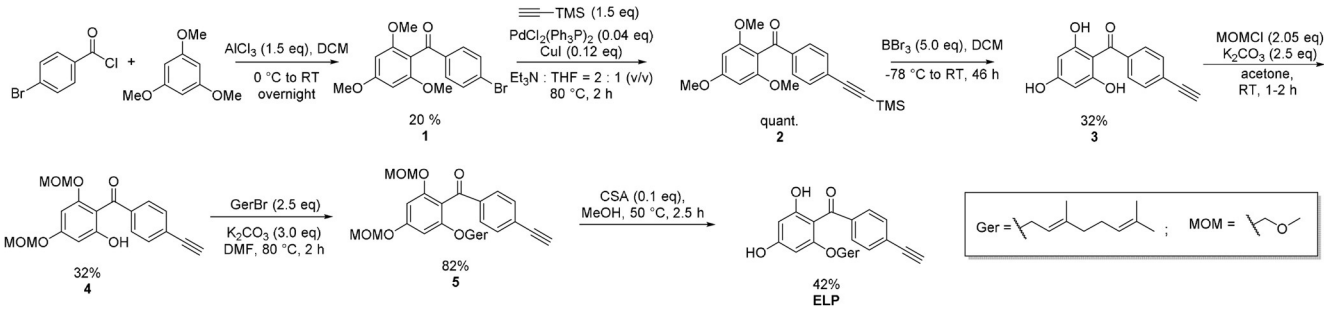

Scheme 1. Synthesis of AfBPP Probe **ELP**. DCM: dichloromethane, RT: room temperature, THF: tetrahydrofuran, DMF: *N*,*N*-dimethylformamide, CSA: camphorsulfonic acid.

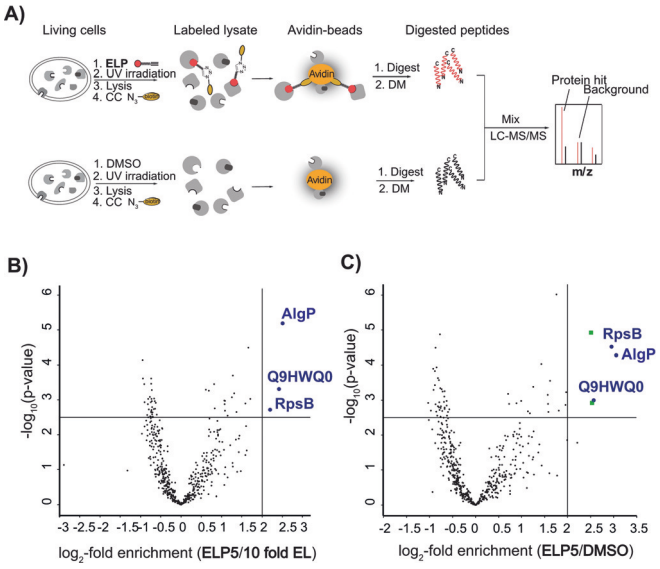

Figure 2. A) Overall scheme of gel-free affinity-based protein profiling (AfBPP) employing isotope labeling. CC: click chemistry; DM: stable isotope dimethyl labeling. B) and C) Volcano plots of gel-free AfBPP experiment in *P. aeruginosa* PAO1 treated with 50 μM **ELP5** vs. a 10-fold excess of **EL** or DMSO, respectively (both soluble fraction). Blue dots represent protein targets that are enriched by treatment with **ELP5** (criteria: $\log_2$-fold enrichment ≥ 2 and $-\log_{10}(p\text{-value}) \geq 2.5$) and outcompeted by **EL** (criteria: $\log_2$-fold enrichment ≥ 2 and $-\log_{10}(p\text{-value}) \geq 2.5$). Green squares denote targets that are enriched by **ELP5** but not outcompeted by **EL** while black dots denote background proteins. For a full list of proteins please refer to the Supporting Information.

labeling[14] and the enrichment by **ELP** was compared to cells treated with DMSO or the inactive probe **ELP2**. Fumarate reductase (Frd), an enzyme involved in important cellular pathways such as anaerobic respiration,[15] was among the most significant hits (Figure S2). In addition, proteins associated with protein synthesis pathways were significantly enriched, including elongation factor Tu (EF-Tu) and 30S ribosomal protein S2 (RpsB). In order to gain more direct insight into target pathways, we performed whole-proteome analysis of **ELP-**treated *E. faecalis* at sub-MIC concentrations. Interestingly, proteins belonging to the V-type ATP synthase and V-type ATPase complexes that are directly associated with Frd-mediated respiration were consistently up-regulated (Figures S3 and S4). By contrast, no direct link to ribosome function could be established, which was further corroborated by a lack of activity of **EL** and derivatives in translation inhibition assays using reconstituted extracts from *Enterococcus rivorum*,[16] a close homologue of *E. faecalis* that displays a comparable MIC value (12.5 μM) (Figure S5).

We next focused on targets of **ELP5** in clinically relevant Gram-negative *P. aeruginosa* via the above described LC-MS/MS platform. Again, 30S ribosomal protein S2 was strongly enriched, accompanied by the transcriptional regulator AlgP and a probable iron sulfur protein. Competition experiments with an excess of **EL** in the presence of the probe confirmed these proteins as specific targets of the natural product (Figure 2B,C and Figure S6). Unlike the study in *E. faecalis*, EF-Tu could not be detected as significantly enriched. While the function of the iron sulfur protein is largely unexplored, AlgP is known as a histone-like protein that may directly or indirectly regulate alginate gene expression.[17] Recombinant AlgP was also labeled by the probe, suggesting direct binding (Figure S7). To further understand AlgP function in more detail, we investigated toxin expression in *algP* transposon mutants. Two mutants (PW9843 and PW9844) were available in the PAO1 transposon mutant library[18] and confirmed by PCR for the correct insertion (Figure S8A). These insertions occur in a region containing multiple KPPA amino acid repeats that are known to facilitate DNA binding and play an important role for AlgP function.[17a] Of note, while a strong attenuation of pyoverdine and a moderate reduction of pyocyanin levels was observed for PW9844, no significant effect was obtained for PW9843, suggesting that this latter insertion may not fully compromise protein function (Figure S8B,C). In addition, dose–response studies with **ELP5** revealed a concentration-dependent decrease of pyocyanin levels for PW9843 and, to a lesser extent, also for PW9844 (Figure S8D). In the case of pyoverdine, PW9843 exhibited behavior similar to that of the wild type in response to **ELP5**, while PW8944 showed almost undetectable expression level in the presence or absence of the compound (Figure S8E). Overall, these results indicate that, in comparison to the PW9843 mutant, the transposon insertion within PW9844 may completely compromise AlgP function and corresponding toxin expression, more prominently for pyoverdine. In order to clarify how this is linked to the **ELP5** phenotype, we selected PW9844 for whole-proteome analysis and comparison with compound-treated cells. Thus, proteomes of *P. aeruginosa* PAO1 treated with **ELP5** and the PW9844 AlgP transposon mutant were analyzed via label-free LC-MS/MS, revealing a striking overall similarity of regulated proteins (Figures S9 and S10). Interestingly, pyoverdine biosynthesis proteins as well as MexGHI-OpmD, a known transporter of phenazines, were strongly downregulated in both samples.[19] By contrast, no pronounced changes for pyocyanin biosynthesis enzymes were observed, suggesting that the lower extracellular levels of this toxin may stem from reduced MexGHI-mediated transport. Taken together, our proteomic profiles confirm a strong link between compound treatment and impairment of AlgP function. However, the differences in pyoverdine levels of PW9844 and compound-treated wild type cells point towards a more complex regulatory function, which needs to be explored in future studies.

Given the importance of *P. aeruginosa* as a pathogen, we selected this bacterium for further evaluation of the **EL** treatment potential.[20] Because **EL**/**ELP5** did not display growth-inhibitory activity on *P. aeruginosa* (Figure 3A), we investigated whether these compounds could be used to potentiate the activity of sub-inhibitory concentrations of antibiotics and thereby facilitate natural bacterial elimination by the host immune system. In vitro infection assays with human THP-1 macrophages demonstrated that the presence of **EL** or **ELP5** enhanced the capacity of sub-inhibitory concentrations of the marketed antibiotic drug norfloxacin to kill intracellular *P. aeruginosa* (Figure 3B). Furthermore, neither **EL** nor **ELP5** were cytotoxic for THP-1 macrophages and we did not observe adverse effects in *Caenorhabditis*

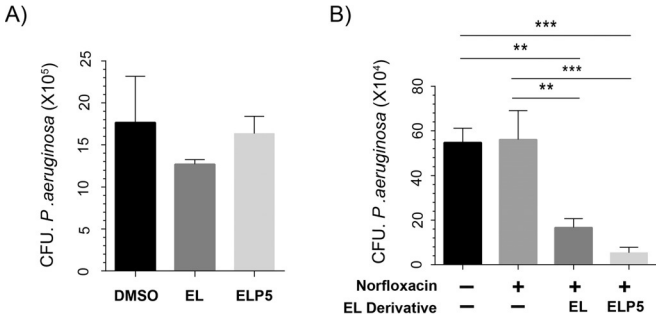

Figure 3. A) Number of viable *P. aeruginosa* PAO1 cells cultured in the presence or absence of 50 μM **EL** or **ELP5** for 5 h. Cultures were inoculated with 5×10^5 *P. aeruginosa* bacteria. B) Intracellular viable *P. aeruginosa* in human THP-1 macrophages. The number of viable intracellular *P. aeruginosa* was determined after lysing the infected THP-1 macrophages. Concentration of **EL** derivatives and norfloxacin was 50 μM and 1.5 μg mL^{-1}, respectively. Each bar represents the mean ± SD of the data from three independent experiments. **, $p<0.05$; ***, $p<0.005$; one-way ANOVA with Tukey's multiple comparison test.

elegans up to a concentration of 300 μM (Figures S11 and S12). Thus, combining **EL**/**ELP5** with an antibiotic can reduce antibiotic doses for the treatment of infection.

In conclusion, we use here the intrinsic photoreactivity of a selected antibacterial natural product with a previously unknown mode of action. In *P. aeruginosa* the compounds appear to mediate inhibition of toxin production via AlgP binding and downregulation of MexGHI, which is responsible for phenazine transport providing a rational for the observed reduction of extracellular pyocyanin levels. Furthermore, the combination of **EL** with sub-inhibitory concentrations of norfloxacin facilitated the killing of intracellular *P. aeruginosa* in macrophages. Given the paucity of compounds active against Gram-negative strains, the low toxicity and unique target profile of **EL** represent an intriguing starting point for further development.

Acknowledgements

The work was funded by grants from the Deutsche Forschungsgemeinschaft (SI-1096/10-1 to S.A.S. and WI3285/6-1 to D.N.W.), by the National Science Foundation CHE1755698 (W.M.W.), and the National Institute of General Medical Sciences GM119426 (W.M.W.). A.R.C. was supported in part by the CF@LANTA RDP Fellowship Program from the Cystic Fibrosis Foundation (MCCART15R0). We thank Dr. Klaus Richter for his kind support for *C. elegans* experiments, Prof. Markus Gerhard for the supply of *S. aureus* clinical isolates, and Sabine Lehne for excellent technical support.

Conflict of interest

The authors declare no conflict of interest.

Keywords: antibiotics · chemical proteomics · natural products · *Pseudomonas aeruginosa* · virulence

How to cite: *Angew. Chem. Int. Ed.* **2019**, *58*, 8581–8584
Angew. Chem. **2019**, *131*, 8670–8674

[1] S. E. Rossiter, M. H. Fletcher, W. M. Wuest, *Chem. Rev.* **2017**, *117*, 12415–12474.
[2] a) M. Lakemeyer, W. Zhao, F. A. Mandl, P. Hammann, S. A. Sieber, *Angew. Chem. Int. Ed.* **2018**, *57*, 14440–14475; *Angew. Chem.* **2018**, *130*, 14642–14682; b) M. F. Chellat, L. Raguz, R. Riedl, *Angew. Chem. Int. Ed.* **2016**, *55*, 6600–6626; *Angew. Chem.* **2016**, *128*, 6710–6738.
[3] S. W. Dickey, G. Y. C. Cheung, M. Otto, *Nat. Rev. Drug Discovery* **2017**, *16*, 457–471.
[4] R. Guerillot, L. Li, S. Baines, B. Howden, M. B. Schultz, T. Seemann, I. Monk, S. J. Pidot, W. Gao, S. Giulieri, A. Goncalves da Silva, A. D'Agata, T. Tomita, A. Y. Peleg, T. P. Stinear, B. P. Howden, *Genome Med.* **2018**, *10*, 63–77.
[5] a) M. J. Evans, B. F. Cravatt, *Chem. Rev.* **2006**, *106*, 3279–3301; b) M. Fonovíc, M. Bogyo, *Expert Rev. Proteomics* **2008**, *5*, 721–730.
[6] K. Bush, P. A. Bradford, *Cold Spring Harbor Perspect. Med.* **2016**, *6*, a025247.
[7] M. H. Wright, S. A. Sieber, *Nat. Prod. Rep.* **2016**, *33*, 681–708.
[8] J. S. Cisar, B. F. Cravatt, *J. Am. Chem. Soc.* **2012**, *134*, 10385–10388.
[9] S. A. Sarkisian, M. J. Janssen, H. Matta, G. E. Henry, K. L. Laplante, D. C. Rowley, *Phytother. Res.* **2012**, *26*, 1012–1016.
[10] W. K. Shiu, M. M. Rahman, J. Curry, P. Stapleton, M. Zloh, J. P. Malkinson, S. Gibbons, *J. Nat. Prod.* **2012**, *75*, 336–343.
[11] T. Rasamiravaka, Q. Labtani, P. Duez, M. El Jaziri, *BioMed Res. Int.* **2015**, *2015*, 759348.
[12] a) G. W. Lau, D. J. Hassett, H. Ran, F. Kong, *Trends Mol. Med.* **2004**, *10*, 599–606; b) S. Jayaseelan, D. Ramaswamy, S. Dharmaraj, *World J. Microbiol. Biotechnol.* **2014**, *30*, 1159–1168.
[13] A. M. King, S. A. Reid-Yu, W. Wang, D. T. King, G. De Pascale, N. C. Strynadka, T. R. Walsh, B. K. Coombes, G. D. Wright, *Nature* **2014**, *510*, 503–506.
[14] P. J. Boersema, R. Raijmakers, S. Lemeer, S. Mohammed, A. J. R. Heck, *Nat. Protoc.* **2009**, *4*, 484–494.
[15] M. Ramsey, A. Hartke, M. Huycke, in *Enterococci: From Commensals to Leading Causes of Drug Resistant Infection* (Eds.: M. S. Gilmore, D. B. Clewell, Y. Ike), Massachusetts Eye and Ear Infirmary, Boston, **2014**.
[16] R. M. Niemi, T. Ollinkangas, L. Paulin, P. Svec, P. Vandamme, A. Karkman, M. Kosina, K. Lindstrom, *Int. J. Syst. Evol. Microbiol.* **2011**, *62*, 2169–2173.
[17] a) W. M. Konyecsni, V. Deretic, *J. Bacteriol.* **1990**, *172*, 2511–2520; b) V. Deretic, W. M. Konyecsni, *J. Bacteriol.* **1990**, *172*, 5544–5554.
[18] a) M. A. Jacobs, A. Alwood, I. Thaipisuttikul, D. Spencer, E. Haugen, S. Ernst, O. Will, R. Kaul, C. Raymond, R. Levy, L. Chun-Rong, D. Guenthner, D. Bovee, M. V. Olson, C. Manoil, *Proc. Natl. Acad. Sci. USA* **2003**, *100*, 14339–14344; b) K. Held, E. Ramage, M. Jacobs, L. Gallagher, C. Manoil, *J. Bacteriol.* **2012**, *194*, 6387–6389.
[19] D. Wolloscheck, G. Krishnamoorthy, J. Nguyen, H. I. Zgurskaya, *ACS Infect. Dis.* **2018**, *4*, 185–195.
[20] a) M. D. Parkins, R. Somayaji, V. J. Waters, *Clin. Microbiol. Rev.* **2018**, *31*, e00019-18; b) H. S. Cheong, C. I. Kang, Y. M. Wi, E. S. Kim, J. S. Lee, K. S. Ko, D. R. Chung, N. Y. Lee, J. H. Song, K. R. Peck, *Am. J. Med.* **2008**, *121*, 709–714.

Manuscript received: March 21, 2019
Accepted manuscript online: April 10, 2019
Version of record online: May 16, 2019

